JOURNAL OF SPACECRAFT AND ROCKETS
Vol. 31, No. 4, July–August 1994

Computation of the Roll Moment for a Projectile with Wrap-Around Fins

Harris L. Edge*
U.S. Army Research Laboratory, Aberdeen Proving Ground, Maryland 21005

Flowfield solutions of a projectile with wrap-around fins have been computed for velocities ranging from Mach 1.3 to Mach 3.0. The flowfield solutions were computed with a time-marching, three-dimensional, zonal, full Navier-Stokes code. The roll moment coefficient was computed from the flowfield solutions and compared to the roll moment coefficient obtained experimentally for a similar wrap-around fin projectile. The roll moment coefficient computations show favorable agreement with experimental measurements in predicting changes of the roll moment coefficient magnitude and sign as a function of the flight Mach number. This demonstrates computational fluid dynamics' capability as a promising method for reliably predicting the roll moment coefficient of projectiles with wrap-around fins.

Nomenclature

C_l = net roll moment coefficient
L = projectile length, 101.6 cm
Re = Reynolds number, $\rho_\infty u_\infty L/\mu_\infty$
u_∞ = freestream velocity
μ_∞ = freestream viscosity
ρ_∞ = freestream density

Introduction

WRAP-AROUND fins have been used primarily for their advantages in packaging tube-launched projectiles. The wrap-around fin conforms to the cylindrical shape of the projectile while in the launch tube, allowing more efficient use of space. Thus, greater numbers of wrap-around fin projectiles can be stored in the same space as fixed-fin projectiles designed to deliver the same payload.[1,2]

The cylindrical shape of the wrap-around fin is advantageous for packaging; but it can also be compromising to the dynamic stability of the projectile. In many configurations where wrap-around fins have been employed, it has been noted that the roll moment coefficient may change in magnitude and sign as the Mach number varies.[1-3] During the course of flight of a wrap-around fin projectile, it is possible for its spin rate to increase or decrease more than once. In addition, the direction of spin may change. This type of behavior can produce poor flight dynamics. To design dynamically stable projectiles employing wrap-around fins, it is necessary to have the ability to predict the roll moment coefficient at all flight conditions for the full trajectory. Design code methodology is inadequate for this problem.[4] Results from computational fluid dynamics (CFD) calculations have shown promise. Normal force coefficients calculated using inviscid CFD computations have compared favorably with experimental data. However, roll moment coefficients calculated using inviscid CFD computations have not shown good agreement with experimental data.[5] This paper presents the initial results for establishing the capability of predicting the roll moment coefficient for a projectile with wrap-around fins through viscous computations with a three-dimensional, full Navier-Stokes code.

Presented as Paper 93-0499 at the AIAA 31st Aerospace Sciences Meeting, Reno, NV, Jan. 11–14, 1993; received Feb. 6, 1993; revision received May 17, 1993; accepted for publication May 20, 1993. This paper is declared a work of the U.S. Government and is not subject to copyright protection in the United States.
*Aerospace Engineer. Member AIAA.

About the Test Case

The experimental data used for comparison were obtained from Refs. 1, 6, and 7. The reports document a comprehensive effort to experimentally determine how changes in geometry affect the aerodynamic forces generated by wrap-around fins. A standard wrap-around fin projectile determined by the Technical Cooperation Program (TTCP), as seen in Fig. 1, was used as the basic configuration. A number of geometric variations to the basic configuration were made. The aerodynamic forces of each configuration were measured and documented. The configuration for the wrap-around fin projectile modeled in the computation was derived from the standard set by the TTCP.[1,6] Although the body retains the dimensions of the standard TTCP configuration, the fins differ slightly. The standard TTCP configuration had fins with symmetric leading and trailing edge bevels. The computational model had blunt leading and trailing edges. There is a difference of 45 deg between the root and tip chord in the standard TTCP configuration while the root and tip chord are parallel in the computational model. Note how the tip chord intersects the 45 deg line in Figs. 2–4 for a visual reference. Another difference to note is that the standard TTCP configuration had boundary layer trips on the body and the fin leading edges.[1,6] The boundary layer was laminar for the body and fins for the computational model.

Flowfield solutions at 0 deg angle of attack were computed for a series of Mach numbers ranging from 1.3 to 3.0 at sea-level atmospheric conditions. The freestream conditions were: density = 1.198 kg/m^3, static temperature = 21.6 °C, and static

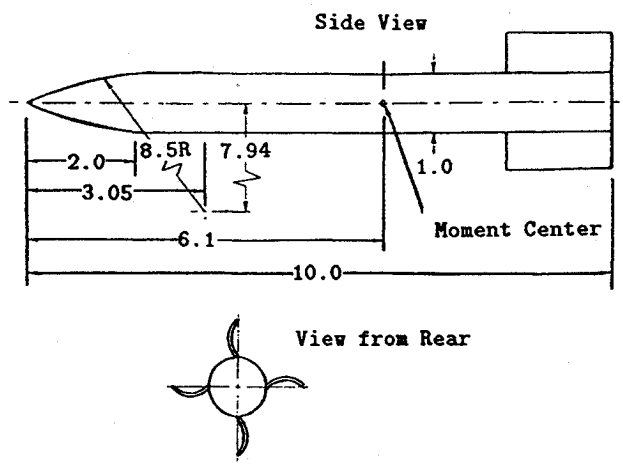

Fig. 1 Wrap-around fin model geometry.

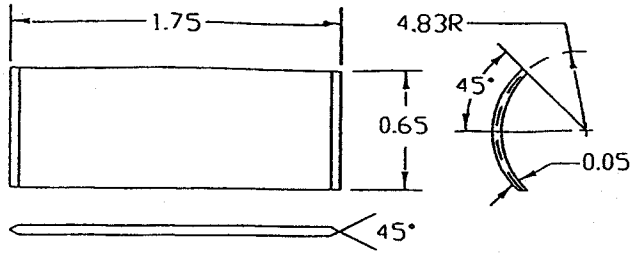

Fig. 2 TTCP standard wrap-around fin.

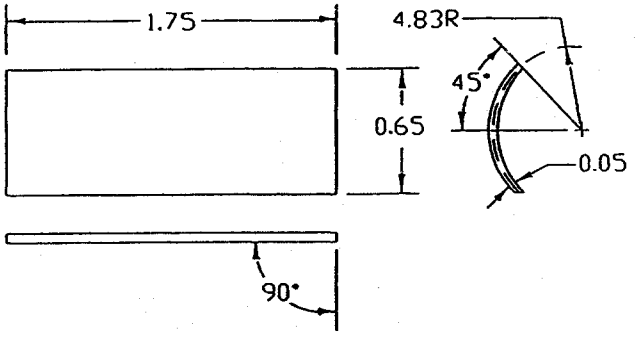

Fig. 3 Blunt leading edge wrap-around fin.

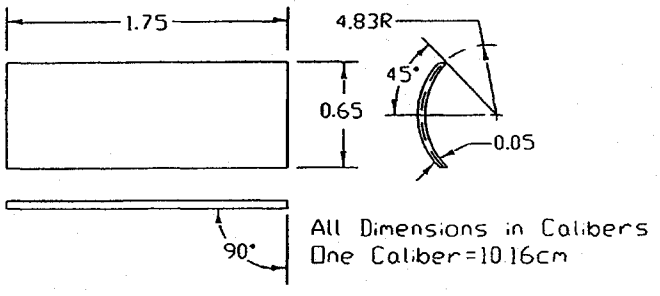

Fig. 4 Computational model wrap-around fin.

pressure = 101.3 kPa. The Reynolds number, based on projectile length, for sea-level conditions ranged from 30 to 69 million. Flowfield solutions were also computed using wind tunnel freestream conditions. The Reynolds number under wind tunnel conditions varied from 17 million at Mach 1.3 to 69 million at Mach 3.0. The wind tunnel atmospheric conditions were obtained from Ref. 7. The experimental data were obtained from four different sites: the McDonnell Douglas Aerophysics wind tunnel, the Arnold Engineering Development Center (AEDC); NASA Langley Research Center, and the Jet Propulsion Laboratory (JPL). The experiments conducted by McDonnell Douglas, AEDC, and NASA Langley were wind tunnel tests while the JPL data were obtained from a free-flight test.[1,6] The models used in the McDonnell Douglas, AEDC, and NASA Langley experiments followed the TTCP specifications. The models used to obtain the experimental data at JPL were approximately 0.15 scale versions of those used for the wind tunnel experiments. These models did not have boundary layer trips on the leading edges of the fins.[1,6] The experimentally obtained roll moment coefficients have been compared to values computed from flowfield solutions calculated by the Ballistic Research Laboratory (BRL) Zonal Navier-Stokes code. Wind tunnel data were available comparing the TTCP standard configuration with a configuration that had blunt leading and trailing edges. See Fig. 3 for this configuration. These data will be discussed later.

Code and Boundary Conditions

All flowfield solutions were computed with the BRL Zonal code. The BRL Zonal code is a three-dimensional, full Navier-Stokes code that can be applied to zonal grid topologies. The governing equations are numerically integrated by an explicit time-marching method.[8,9]

The flowfield solutions were viscous flow calculations. The computationally modeled surface was one-fourth of the entire projectile surface. The symmetry of the projectile allowed the modeling of one fin and approximately 45 deg of body surface on either side of the fin. A periodic boundary condition was written to take advantage of this symmetry. This helped to reduce the number of grid cells needed for the computation, but it restricted the angle of attack to zero degrees. The calculation of the roll moment coefficient was the primary goal in this initial effort. For this reason, the flowfield was computed for the body and fins only, since the influence of the recirculating flow at the base on the roll moment coefficient is expected to be small. Future computations which include flowfield solutions at the projectile base will hopefully verify the accuracy of this assumption. A zero gradient boundary condition was used at the trailing edges of the fins for the downstream boundary condition. A nonreflecting boundary condition was applied to the outermost grid plane from the body surface. The nonreflecting boundary condition allowed the outermost grid plane to be placed relatively close to the body, which reduced the number of computational points needed for a solution. In order to obtain a viscous solution, the fin and body surfaces were modeled with a no-slip boundary condition.

A zonal approach was used to obtain a solution for the flowfield. In the zonal approach, as implemented in the BRL Zonal code, overlapped zones share at least one grid cell in a given direction with an adjacent zone. The shared grid cells have identical coordinates in both of the overlapped zones. Since the two overlapped zones have the same coordinates for the shared grid cells, zonal coupling requires only the transfer of information from the field of one zone to the boundary of the other zone and vice versa. No interpolation is required. A multizone solution is obtained by performing the integration of the governing equations in all zones and then exchanging information between overlapping zones before advancing to the next iteration.[8,9]

All computations were performed on a Cray-2 supercomputer. Some flowfield solutions were computed on the TACOM Cray-2 while others were computed on the Cray-2 at BRL. As configured for this case, the BRL Zonal code required 45 million words of memory.

Computational Grid

The zonal approach facilitated the building of the computational grid. The unswept wrap-around fins with blunt leading edges would have been difficult to model with a wrap-around grid. The use of a wrap-around grid would have resulted in large and rapid variations of the metric terms, which could have severely degraded the quality of the solution.[8,9] The zonal approach allowed the accurate modeling of the wrap-around fin projectile's geometry while retaining a smooth, continuous

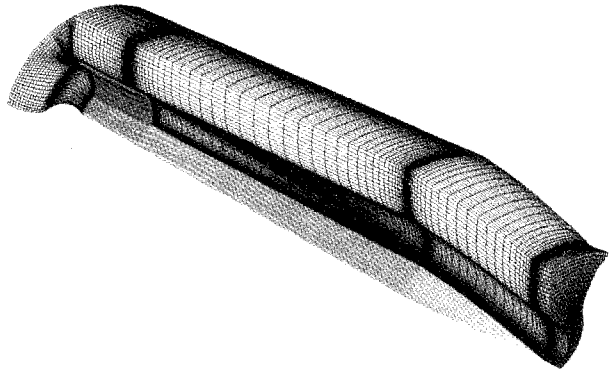

Fig. 5 Computational grid.

computational mesh. A cut-away view of the computational grid can be seen in Fig. 5.

The grid was designed for viscous computation. It was highly clustered near the body and fin surfaces. The total number of points used for the computation was 951,888. The dimensions for each of the seven zones were as follows: (20 × 80 × 32), (20 × 80 × 32), (130 × 80 × 32), (130 × 80 × 32), (20 × 80 × 18), (96 × 80 × 18), (36 × 26 × 48). As stated earlier, these seven zones were configured to model one-fourth of the wrap-around fin projectile.

An algebraic grid generator, developed at BRL, was used to build the computational mesh. Once the interior mesh of a zone is completed, grid points on the boundary are added, deleted or changed to create overlaps between adjacent zones. For the periodic boundary condition to function properly, the planes in which data were exchanged were spaced such that they were exactly ninety degrees apart in the circumferential direction.

Results

Qualitatively, the flowfield solutions computed by the BRL Zonal code show a number of interesting features of wrap-around fin aerodynamics. Figures 6–8 show surface pressure contours on the concave and convex sides of the wrap-around fins at different Mach numbers. These figures show the influence of shocks generated at the fin leading edge on the fin surface. In addition, the figures also show the development of a high-pressure region near the leading edge of the concave side of the fin as the Mach number increases.

The differences in the surface pressure contours on the convex and concave sides of the fin are quite evident. Figure 9 is a view of the wrap-around fin from its concaveside. Figure 10

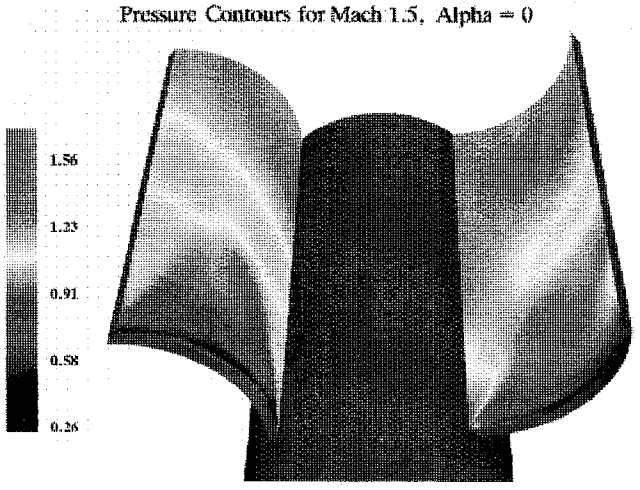

Fig. 6 Normalized pressure contours at Mach = 1.5, Alpha = 0.

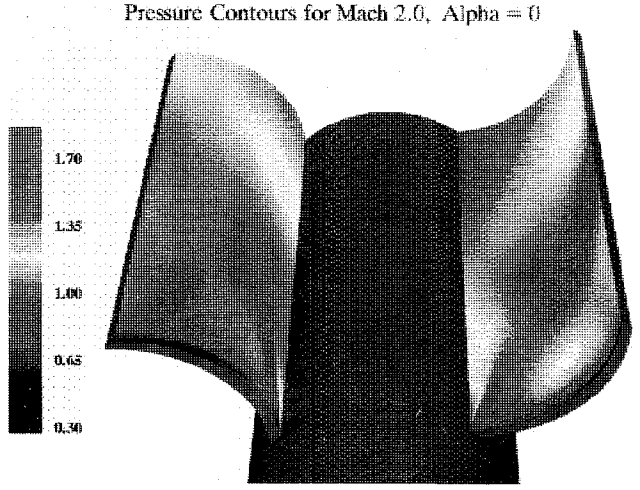

Fig. 7 Normalized pressure contours at Mach = 2.0, Alpha = 0.

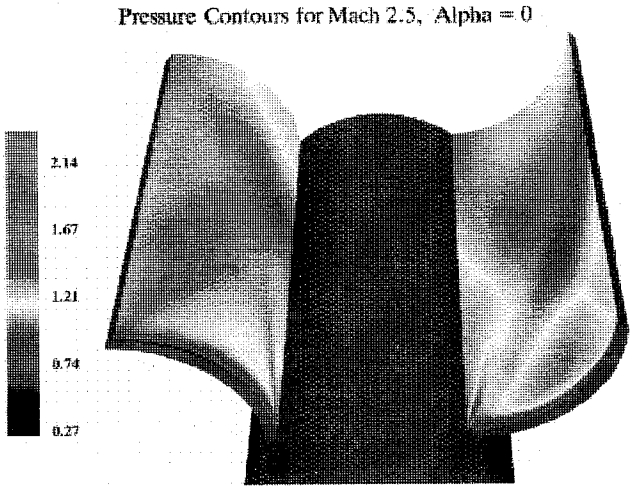

Fig. 8 Normalized pressure contours at Mach = 2.5, Alpha = 0.

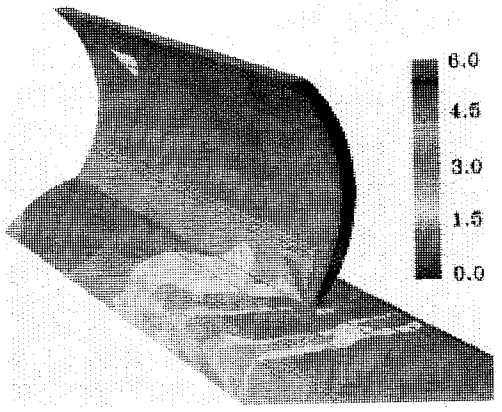

Fig. 9 Normalized pressure contours on concave side of fin at Mach = 2.

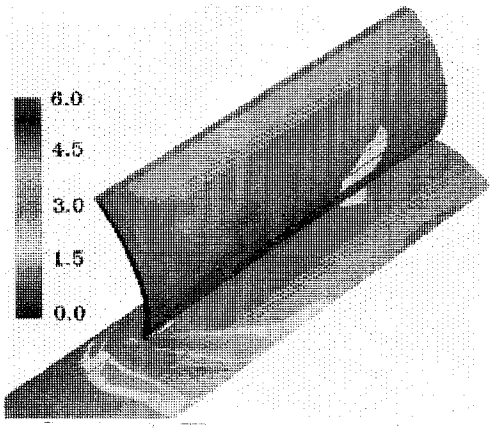

Fig. 10 Normalized pressure contours on convex side of fin at Mach = 2.

is a view from the convex side. Figure 11 shows a view between the fins. Near the fin root, the shock generated by the fin is clearly asymmetric. Figure 12 shows a flowfield plane away from the body that intersects the fin at approximately fifty percent of its height. It should be noted that the plane is not at a constant radial distance from the body surface. The shock on the concave and convex sides of the fin appear to be very similar to each other at a distance away from the body. Near the fin leading edge, at the root of the fin surface pressure on the concave and convex sides of the fin appear to be very different from each other.

Figure 13 shows the flowfield at various axial stations along the fin length. These contours give a good indication of the

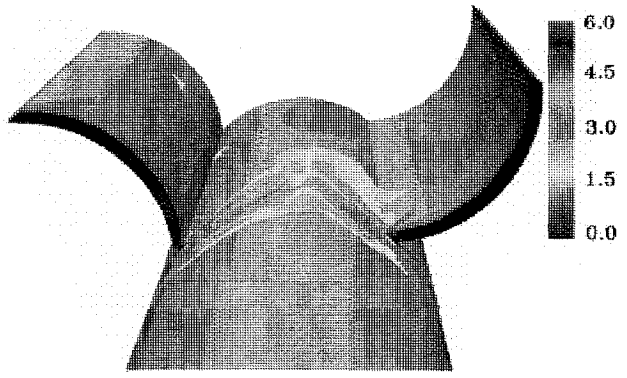

Fig. 11 Normalized pressure contours between fins at Mach = 2.0.

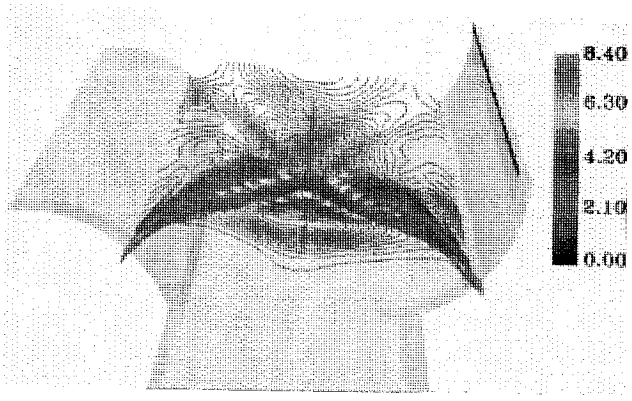

Fig. 12 Normalized pressure contours between fins at Mach = 2.5.

overall structure of shocks generated by a wrap-around fin projectile. The contours also show near the fin surface, the pressure increases towards the fin center of curvature on the concave side of the fin. This is most apparent near the leading edge of the fin. Generally speaking, the leading edge is the area where there is the greatest difference in pressure between the concave and convex sides of the fin. This is in agreement with the findings mentioned in Ref. 1.

A comparison of the computed roll moment coefficient and the experimentally obtained roll moment coefficient shows good agreement with overall trends. Figure 14 is a graph showing the roll moment coefficient vs Mach number for experimental data obtained at JPL and computations made from the BRL Zonal code solutions. Figure 14 shows that the roll moment coefficients computed from BRL Zonal code flowfield solutions follow the general trends of the experimental data. At lower Mach numbers, the roll moment coefficient is positive. At higher Mach numbers, the roll moment coefficient is negative. A positive roll moment coefficient indicates a roll direction towards the fin's center of curvature. The predicted and JPL-measured roll moment coefficients indicate one crossover point, a Mach number at which the roll moment coefficient is zero, near Mach 1.7.

It is expected that the geometrical differences between the computational model and the TTCP standard configuration would produce differences in their roll moment coefficients. Additional wind tunnel data are presented to show how the fin bluntness affects the roll moment coefficient. Figure 15 is a roll moment coefficient vs Mach number plot for two wrap-around fin configurations obtained under similar conditions. One configuration is the standard TTCP configuration while the second configuration is a modified TTCP configuration which has blunt fin edges. Figure 3 shows the fin geometry of this second configuration. The data are presented because the fin leading edge bluntness is the primary geometrical difference between the TTCP standard configuration and the computational model. As can be seen in Fig. 15, the roll moment coefficient vs Mach number curve of the blunt-finned configura-

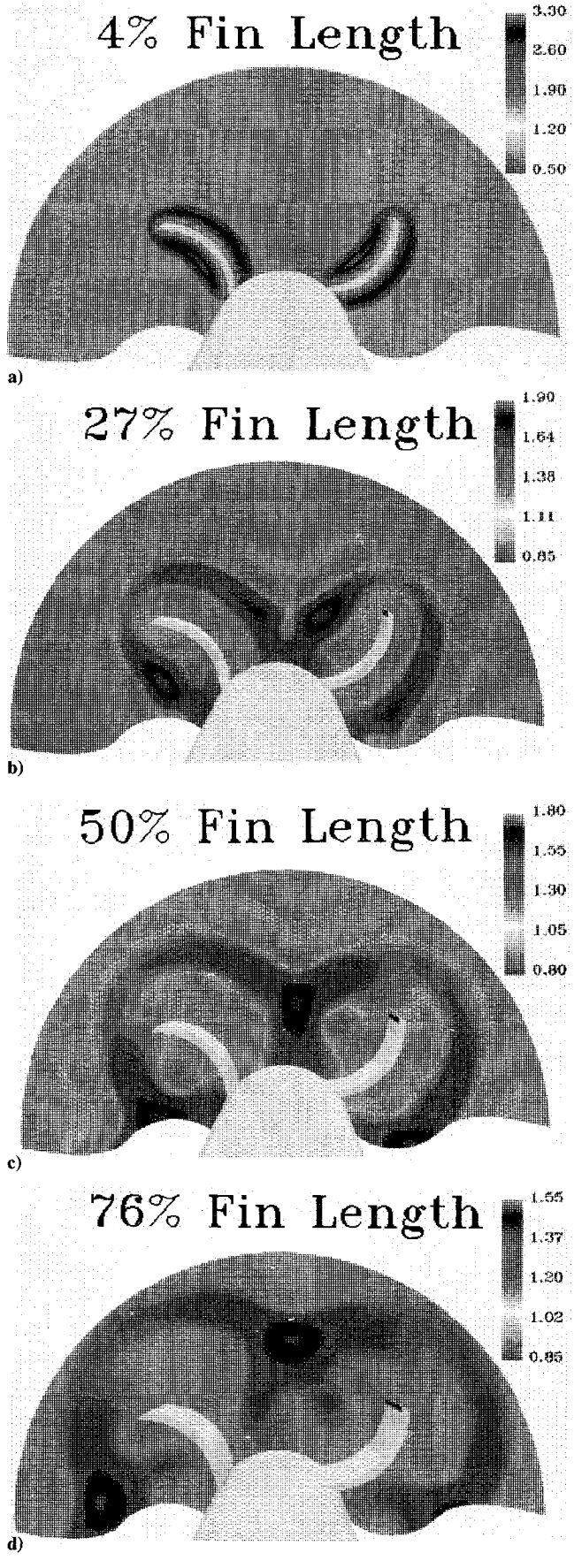

Fig. 13 Normalized pressure contours at various axial stations at Mach = 2.5, and fin lengths of a) 40%, b) 27%, c) 50%, and d) 76%.

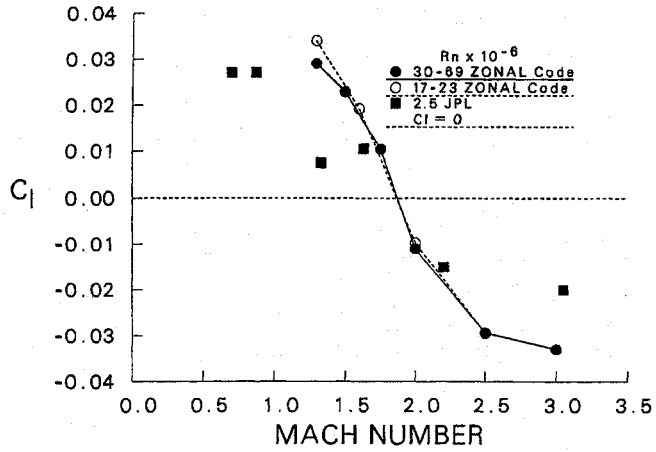

Fig. 14 Roll moment coefficient vs Mach number for computational and JPL experimental data.

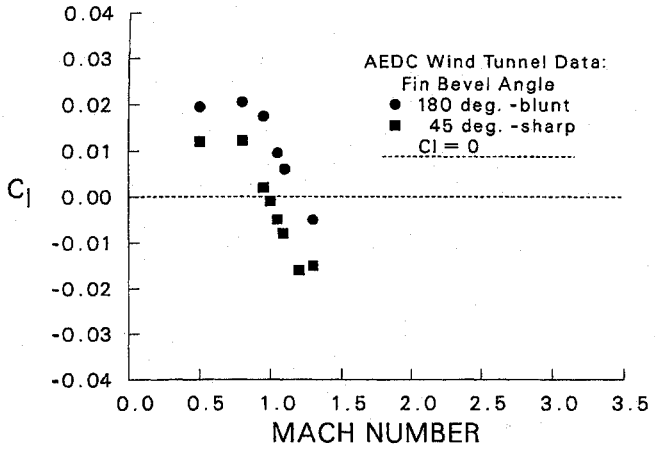

Fig. 15 Roll moment coefficient vs Mach number for configurations with different leading edge bluntness.

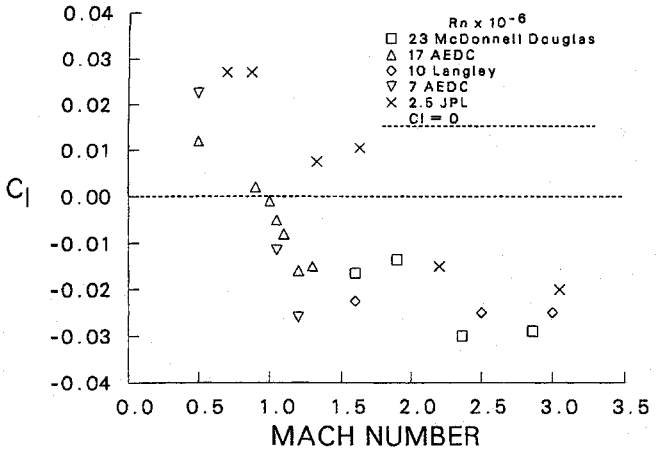

Fig. 16 Roll moment coefficient vs Mach number for experimental data.

tion seems to retain the same overall characteristics of the curve for the TTCP standard configuration. The differences in the two curves indicate that a blunt leading edge as opposed to a forty-five degree leading edge wrap-around fin will have a slightly higher crossover point and, subsonically at least, have a greater roll moment coefficient.

A comparison of the different roll moment coefficients of a standard TTCP configuration obtained from various facilities shows some scatter in the data, but the overall trends stated earlier, remain intact. Figure 16 is a plot of roll moment coefficient vs Mach number for experimental data obtained using the TTCP standard configuration. As stated earlier, the McDonnell Douglas, AEDC, and Langley data were obtained from wind tunnel experiments with the standard TTCP configuration. The JPL free-flight data were obtained using a scaled-down version of the TTCP standard configuration. The model used at JPL did not have boundary layer trips on the fin leading edges while the models used at McDonnell Douglas, AEDC, and Langley did have fin leading edge boundary layer trips.[1,6] In the Dahlke 1975 and 1976 reports, the data in Fig. 16 were presented with a discussion of the effects of Reynolds number on roll moment coefficient. The experimental data indicate that the Reynolds number may have an effect on the roll moment coefficient and Dahlke speculated the Reynolds number and the lack of boundary layer trips may be responsible for the difference in the JPL data and the other experimental data. The JPL data predicts the crossover point to be at approximately Mach 1.7 while the other wind tunnel data indicates Mach 1.0. With the exception of the differing crossover points, the JPL data agrees well with the other wind tunnel data. The computed roll moment coefficients, shown in Fig. 14, indicate that there is little difference in the roll moment coefficient under wind tunnel (Reynolds number 17 to 23 million) and sea level (Reynolds number 30 to 69 million) conditions.

Concluding Remarks

Flowfield solutions of a wrap-around fin projectile were calculated with the BRL three-dimensional Zonal Navier-Stokes code. The roll moment coefficient was calculated from the flowfield solutions and compared to the roll moment coefficient obtained from experiment measurements for a similar wrap-around fin projectile configuration. The computed roll moment coefficients predicted the same trends seen in the experimentally obtained roll moment coefficients in magnitude and sign, (direction). Experimental data obtained from McDonnell Douglas, AEDC, and NASA Langley wind tunnels indicated that the crossover point was at Mach 1 while the JPL free-flight data indicated that the crossover point was greater than Mach 1.0. It is encouraging that the computed roll moment coefficient crossover point was close to the crossover point of the JPL free-flight data. The boundary layer was laminar on the fins in the computational model. Also, the model used for the JPL experiments did not have a boundary layer trip on the fin leading edge, while the models used in the wind tunnel experiments did. Another point to note is that the JPL experiments had the lowest Reynolds number. This raises the possibility that the wrap-around fins of the JPL model may have had a laminar boundary layer at low Mach numbers which would give this experiment another feature in common with the computation. The experimental data indicate that the roll moment coefficient varies with the Reynolds number. However, the data do not establish any trends which would allow one to state conclusively whether there is a relationship between the Reynolds number and roll moment coefficient or what that relationship may be. The results from the CFD computations do not indicate that the roll moment coefficient is Reynolds number dependent.

The roll moment coefficient computations have shown good agreement, in terms of the magnitude and sign, with values of the roll moment coefficient obtained experimentally. The computational technique, as outlined in this report, has shown great promise in being a reliable method for predicting the roll moment coefficient. However, a one-to-one comparison of computation and experiment is difficult to make. As this is an ongoing effort, further work will be done to fully establish this capability. Future plans include applying the F3D code to wrap-around fin configurations,[10] computing turbulent viscous flowfield solutions, and computing flowfield solutions for small angles of attack.

References

[1] Dahlke, C. W., "A Review and Status of Wrap-Around Fin Aerodynamics," *Tenth Navy Symposium on Aeroballistics*, Vol. 1, No. 10,

Naval Surface Weapons Center, Dahlgren Lab., Dahlgren, VA, July 1975, pp. 279–324.

[2] Winchenbach, G. L., Buff, R. S., Whyte, R. H., and Hathaway, W. H., "Subsonic and Transonic Aerodynamics of a Wraparound Fin Configuration," *Journal of Guidance and Control,* Vol. 9, No. 6, 1986, pp. 627–632.

[3] Mermagen, W. H., and Oskay, V., "Yawsonde Tests of 2.75-Inch Mk66 Mod 1 Rocket," U.S. Army Ballistic Research Lab. Rept. ARB-RL-MR-03127, Aberdeen Proving Ground, MD, Aug. 1981.

[4] Dahlke, C. W., and Batiuk, G., "Hydra 70 MK66 Aerodynamics and Roll Analysis," U.S. Army Missile Command, TR RD-SS-90-6, Redstone Arsenal, AL, July 1990.

[5] Wardlaw, A. B., Priolo, F. J., and Solomon, J. M., "Multiple-Zone Strategy for Supersonic Missiles," *Journal of Spacecraft and Rockets,* Vol. 24, No. 4, 1987, pp. 377–384.

[6] Dahlke, C. W., "The Aerodynamic Characteristics of Wrap-Around Fins at Mach Numbers of 0.3 to 3.0." U.S. Army Missile Command, TR RD-77-4, Redstone Arsenal, AL, Oct. 1976.

[7] Humphery, J. A., and Dahlke, C. W., "A Summary of Aerodynamic Characteristics for Wrap-Around Fins from Mach 0.3 to 3.0," U.S. Army Missile Command, TR TD-77-5, Redstone Arsenal, AL, March 1977.

[8] Patel, N. R., Sturek, W. B., and Smith, G. A., "Parallel Computation of Supersonic Flows Using a Three-dimensional, Zonal, Navier-Stokes Code," U.S. Army Ballistic Research Lab. Rept. BRL-TR-3049, Aberdeen Proving Ground, MD, Nov. 1989.

[9] Patel, N. R., and Edge, H. L., "Computations of Integrated Inlet-Combustor Flows for National Aerospace Plane Engine." U.S. Army Ballistic Research Lab. Rept. BRL-IMR-3049, Aberdeen Proving Ground, MD, Feb. 1991.

[10] Sahu, J., "Numerical Computations of Transonic Critical Aerodynamic Behavior," U.S. Army Ballistic Research Lab. Rept. BRL-TR-2962, Aberdeen Proving Ground, MD, Dec. 1988.

Jerry M. Allen
Associate Editor